Emission of correlated photon pairs from superluminal perturbations in dispersive media

F. Dalla Piazza,[1] F. Belgiorno,[3] S. L. Cacciatori,[1,2] and D. Faccio[1,4]

[1]*Dipartimento di Scienza e Alta Tecnologia, Università dell'Insubria, Via Valleggio 11, IT-22100 Como, Italy,*

[2]*I.N.F.N., Sezione di Milano, Via Celoria 16, 20133, Milano, Italy*

[3]*Dipartimento di Matematica, Politecnico di Milano, Piazza Leonardo 32, 20133 Milano, Italy*

[4]*School of Engineering and Physical Sciences, SUPA, Heriot-Watt University, Edinburgh EH14 4AS, United Kingdom*

(Received 12 January 2012; published 27 March 2012)

We develop a perturbative theory that describes a superluminal refractive perturbation propagating in a dispersive medium and the subsequent excitation of the quantum vacuum zero-point fluctuations. We find a process similar to the anomalous Doppler effect: Photons are emitted in correlated pairs and mainly within a Cerenkov-like cone, one on the forward and the other in backward directions. The number of photon pairs emitted from the perturbation increases strongly with the degree of superluminality and under realizable experimental conditions; it can reach up to $\sim 10^{-2}$ photons per pulse. Moreover, it is, in principle, possible to engineer the host medium so as to modify the effective group refractive index. In the presence of "fast-light" media, e.g., a with group index smaller than unity, a further $\sim 10\times$ enhancement may be achieved and the photon emission spectrum is characterized by two sharp peaks that, in future experiments, would clearly identify the correlated emission of photon pairs.

DOI: 10.1103/PhysRevA.85.033833 PACS number(s): 42.50.Ct, 42.65.−k, 12.20.Ds

I. INTRODUCTION

Since the analysis of Schwinger [1] a great amount of research has been devoted to the study of particle production from the vacuum. In a seminal paper [2], Hawking predicted that the presence of a horizon around a black hole induces particle production. Actually, the existence of Hawking radiation does not require a gravitational collapse, but, rather, the key elements are a quantum field and an event horizon associated with a curved space-time metric [3–7]. Another mechanism providing particle production is the dynamical Casimir effect [8]. There, a two-dimensional quantum theory of a massless scalar field is considered that is influenced by the motion of a perfectly reflecting boundary (mirror). The vacuum expectation value of the energy-momentum tensor for an arbitrary mirror trajectory shows a nonvanishing radiation flux.

Here we consider a further effect by which particle production is induced by the superluminal motion of a perturbation of the refractive index in a dielectric medium with dispersion. Differing from the Hawking effect, the production of particles is not induced by the presence of a horizon but by the fast motion of the perturbation. Therefore, this effect can be better recognized in the context of the anomalous Doppler effect [9–12]. Following the description given by Ginzburg, light emitted by a generic moving source will be Doppler shifted according to the formula $\omega(\theta) = \omega'/\gamma|1 - v/cn(\omega)\cos\theta|$ [12], where ω' is the comoving reference frame value of the emitted frequency, θ is the observation angle and $\gamma = 1/\sqrt{1 - v^2/c^2}$. For $v/cn(\omega)\cos\theta < 1$ we have the normal Doppler effect but for $v/cn(\omega)\cos\theta > 1$, i.e., for a superluminal source we have the so-called anomalous Doppler effect (see Fig. 1). Emission of a photon on behalf of the moving source must, in general, correspond to a change in the internal state, e.g., a transition in energy from one level to another. In the normal Doppler regime, a positive-frequency photon, thus, will be emitted with a spontaneous transition from an upper to a lower energy state. In much the same way, in the anomalous Doppler regime a negative-frequency photon (positive frequency in the laboratory reference frame) will be spontaneously emitted in combination with a transition from a lower to a higher state. The energy required for this process is provided by the superluminal translational movement. Therefore, the superluminal source will continuously emit pairs of photons, one in the anomalous and the other in the normal Doppler regions [12]. Anomalous Doppler emission has never actually been observed before due to the obvious difficulty in actually realizing an experimental system in which to observe these effects.

In this work we extend the same concept proposed to generate event horizons in optical media: An intense laser pulse focused into the medium will induce a local increase in the refractive index and this create a perturbation in the dielectric medium (PDM) that travels locked with the laser pulse itself [5,7]. Laser pulses will typically travel at a well-defined group velocity so this kind of PDM is ideal for creating the analog of an event horizon. However, by properly choosing how the laser pulse overlaps with the dielectric medium, it is possible to generate a PDM that travels with any arbitrary velocity. For example, recent experimental results clearly show that it is possible to generate isolated peaks within the laser pulse that travel faster than the vacuum speed of light, c [13,14]. Within the context of these findings we, therefore, consider the problem of how a superluminal PDM interacts with the zero-point fluctuations of the surrounding quantum vacuum. This same problem was first tackled in Ref. [15], where it was shown that, in a dispersion-less medium, a superluminal PDM will spontaneously emit photons that are excited from the vacuum state. The photons appear as correlated pairs and their wavelength decreases from the far-infrared to the visible region as the PDM velocity is increased from $\sim c$ to many times c. Here we extend these results to a dispersive medium and we consider in more detail the nature of the correlated photons and possible experimental implementation. We also consider how the correlated photon pair emission may be enhanced by properly engineering the vacuum states, i.e., by using media in which the effective group velocity at the

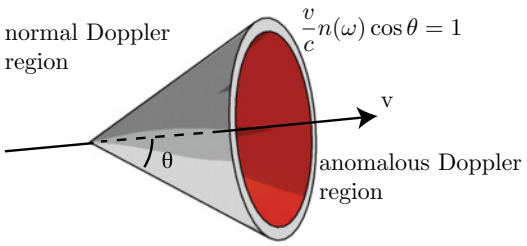

FIG. 1. (Color online) Schematical representation of normal and anomalous Doppler emission from a "source" moving with velocity v.

emitted frequencies is also superluminal, so-called fast-light media [16].

II. NONDISPERSIVE CASE

We start by briefly summarizing the main results and equations for the nondispersive case treated in Ref. [15].

An intense light pulse induces the perturbation of the refractive index through the optical nonlinear Kerr effect. This perturbation travels across the medium at the same speed of the light pulse. The medium was supposed to be nondispersive. The authors find that there is no pair production unless the pulse velocity v satisfies the condition $v \geqslant \frac{c}{n_0}$, where c is the velocity of light in vacuum end n_0 is the uniform and constant background refraction index. The model analyzed is based on the perturbative approach introduced by Schützhold *et al*. in Ref. [17] and the interaction representation for the electromagnetic field in the presence of a dielectric constant $\epsilon(\vec{x},t)$ depending on space and time is considered. Moreover, a uniform background and a constant value $\epsilon_b = n_0^2$ for the dielectric constant are assumed. Thus, the disturbance is $\epsilon(\vec{x},t) - \epsilon_b$. Following Ref. [17], the interaction Hamiltonian is $\mathcal{H}_I = \xi\,\Pi^2$ with $\xi := \frac{1}{2}[\frac{1}{\epsilon(\vec{x},t)} - \frac{1}{\epsilon_b}]$ and the number of particles created, labeled by the momentum $\vec{k}$ and the polarization μ, is

$$N_{\vec{k}_1\mu_1} = \sum_{\vec{k}_2} \frac{\omega_1\omega_2}{V^2}|\tilde{\xi}(\underline{k}_1 + \underline{k}_2)|^2\left[1 - \left(\vec{e}_{\vec{k}_2}\cdot\vec{e}_{\vec{k}_1\mu_1}\right)^2\right], \quad (1)$$

where $\underline{k} = (\vec{k},\omega_{\vec{k}}) = (\vec{k},ck/n_0)$, with $k = |\vec{k}|$, $\vec{e}_{\vec{k}} = \vec{k}/k$, the subscripts 1 and 2 label the particles of the emitted couple, and the particular shape of the perturbation is contained in the function ξ. Considering a Gaussian behavior for the refraction index $n^2 = \epsilon(x,t,y,z)$,

$$n^2 = n_0^2 + 2n_0\eta e^{-[(x-vt)^2+y^2+z^2]/2\sigma^2}, \quad (2)$$

the expression for the number of created particles becomes [18]

$$N_{\vec{k}_1,\mu_1} = 2^2\sigma^6\frac{\pi^2}{v^2}\frac{\eta^2}{n_0^6}\int d\vec{k}'\frac{\omega_1\omega_2}{V}e^{-\sigma^2|\vec{k}_1+\vec{k}_2|^2}\left[\delta\left((\vec{k}_1+\vec{k}_2)_x - \frac{c}{vn_0}(k_1+k_2)\right)\right]^2\left[1-\left(\vec{e}_{\vec{k}_2}\cdot\vec{e}_{\vec{k}_1\mu_1}\right)^2\right]. \quad (3)$$

The δ function gives a constraint on the possible values of the momenta for the emitted particles.

III. DISPERSIVE CASE

A. Perturbation

When considering actual experiments, the previous model should only be considered as an approximation of a real medium and one has to take into account the presence of the dispersion. In this section we generalize the model of Ref. [15] for dispersive media. To introduce dispersion in the model we have to refine the approach leading to the expression for the number of emitted particles. The first step, up to Eq. (19), is to derive the Hamiltonian for a superluminal perturbation in a dispersive medium. This Hamiltonian will then be used, in a similar fashion to the treatment in Ref. [15], to derive the number of particles excited out of the vacuum state. Let us write the dispersive electromagnetic action as [19]

$$S = \frac{1}{2}\int \vec{E}\cdot\varepsilon\vec{E}dx^4, \quad (4)$$

where $\varepsilon\vec{E}$ is

$$\varepsilon\vec{E}(\vec{r},t) = \varepsilon(\vec{r},i\partial_t)\vec{E}(\vec{r},t). \quad (5)$$

The variation of the action [Eq. (4)] with respect to the potential related to the electric field, E, gives the Maxwell equations, with no free charges, for E. We will not specify the operator ε now, but we will assume for it to be a symmetric operator. We will also assume that its inverse operator ε^{-1} exists. The unperturbed canonically conjugate momentum is then

$$\vec{\Pi} = \varepsilon\vec{E}, \quad (6)$$

as can be computed from Eq. (4) using the Lagrangian formalism. If we expand in Fourier series the electric field and the conjugate momentum as

$$\vec{E}_\omega(\vec{r}) = \int_{\mathbb{R}} e^{-i\omega t}\vec{E}(\vec{r},t)dt, \quad (7)$$

$$\vec{\Pi}_\omega(\vec{r}) = \int_{\mathbb{R}} e^{-i\omega t}\vec{\Pi}(\vec{r},t)dt, \quad (8)$$

we can write

$$\vec{E} = \varepsilon^{-1}\vec{\Pi} = \frac{1}{2\pi}\int_{\mathbb{R}} e^{i\omega t}\frac{1}{\varepsilon(\vec{r},\omega)}\vec{\Pi}_\omega(\vec{r})d\omega. \quad (9)$$

We introduce a perturbation $\varepsilon(\vec{r},i\partial_t) \mapsto \varepsilon(\vec{r},i\partial_t) + \delta\varepsilon(\vec{r} - \vec{v}t,i\partial_t)$. To proceed, we note that now the momentum is

$$\vec{\Pi} = \varepsilon\vec{E} + \delta\varepsilon\vec{E}. \quad (10)$$

To describe the Hamiltonian we have to invert this operator in order to express the electric field in terms of the momentum. This can be done perturbatively. The perturbative series expansion is expressed in terms of a (small) parameter η so

$$\delta\varepsilon(\vec{r} - \vec{v}t,i\partial_t) = \eta\varepsilon_1(\vec{r} - \vec{v}t,i\partial_t). \quad (11)$$

We next write

$$\vec{E} = \vec{E}_0 + \eta\vec{E}_1 + \cdots, \quad (12)$$

where the dots are higher orders in η. We then have

$$\vec{\Pi} = \varepsilon\vec{E}_0 + \eta(\varepsilon_1\vec{E}_0 + \varepsilon\vec{E}_1), \quad (13)$$

where we have neglected the term $\eta\delta\varepsilon E_1 = \eta^2\varepsilon_1 E_1$ being of second order in η. Equation (13), compared with Eq. (6) at the

first order, gives

$$\vec{\Pi} = \varepsilon \vec{E}_0, \tag{14}$$

$$\varepsilon \vec{E}_1 = -\varepsilon_1 \vec{E}_0. \tag{15}$$

Therefore, we may quantize the theory perturbatively by using the unperturbed momentum operator $\vec{\Pi}$ and the perturbation

$$\delta \vec{E} = \eta \vec{E}_1 = -\varepsilon^{-1}(\delta\varepsilon \vec{E}_0) = -\varepsilon^{-1}(\delta\varepsilon\ \varepsilon^{-1}\vec{\Pi}). \tag{16}$$

We now calculate the integral of the whole space-time of the Hamiltonian density by taking the Legendre transformation of the action. Using the expression for the unperturbed momentum and of the perturbation, the Legendre transformation is

$$\begin{aligned}\frac{1}{2}\int \vec{\Pi}\cdot\vec{E}dx^4 &= \frac{1}{2}\int \vec{\Pi}\cdot\varepsilon^{-1}\vec{\Pi}dx^4 \\ &\quad -\frac{1}{2}\int \vec{\Pi}\cdot\varepsilon^{-1}(\delta\varepsilon\ \varepsilon^{-1}\vec{\Pi})dx^4 + \cdots \\ &= \frac{1}{2}\int \vec{\Pi}\cdot\varepsilon^{-1}\vec{\Pi}dx^4 \\ &\quad -\frac{1}{2}\int \varepsilon^{-1}\vec{\Pi}\cdot\delta\varepsilon\ \varepsilon^{-1}\vec{\Pi}dx^4 + \cdots,\end{aligned} \tag{17}$$

where the dots are higher-order terms and we have used the symmetry of ε^{-1} (and dropped total time derivatives).

Thus, the Hamiltonian density is

$$\mathcal{H} = \mathcal{H}_0 + \mathcal{H}_I, \tag{18}$$

where $\mathcal{H}_0$ is the unperturbed Hamiltonian (with dispersion) and

$$\mathcal{H}_I := -\tfrac{1}{2}\varepsilon^{-1}\vec{\Pi}\cdot\delta\varepsilon\ \varepsilon^{-1}\vec{\Pi} \tag{19}$$

is the first-order perturbation, which reduces to the Hamiltonian used in Refs. [15,17] in the absence of dispersion.

The perturbative computation is then carried forward starting from this expression, and, as in the nondispersive case, we adopt the interaction representation.

IV. THE MODEL

Consider a perturbation of the refractive index moving in the x direction with velocity v, i.e., $n(\omega) + \delta n(x - vt)$ and assume that the ω dependence of the term δn is negligible. Thus, at the first order in δn the dielectric constant is $\epsilon(\omega)^2 + 2n(\omega)\delta n(x - vt)$. The perturbation term (19) may be taken as an operator that we can write formally (from now on we will omit the subscript 0) as

$$\mathcal{H}_I = -\tfrac{1}{2}\vec{E}\varepsilon_1\vec{E} = -\vec{E}\,[n(i\partial_t)\delta n(x - vt)]^S\,\vec{E}, \tag{20}$$

where the apex S implies the Weyl prescription for the maximally symmetrized operator [20]. The perturbative approach used here may be justified by evaluating the main parameters under investigation. We expect to observe a similar behavior to the nondispersive case for which there is a peak of emission for $\lambda_{\max} = 3\sigma$ [15], where σ is the radius of the Gaussian-shaped perturbation. It is reasonable to expect that the perturbative approach works if the measured wavelength λ satisfies $\sigma/\lambda >> \eta$. For example, if η is of the order of 0.01–0.001 the perturbative approach is justified for emitted wavelengths well below 100 nm if $\sigma \sim 1\ \mu$m. In this situation the operator appearing in Eq. (20) can be approximated by the more tractable one, $-\frac{1}{2}\vec{E}\varepsilon_1\vec{E} = -\vec{E}\,(n(i\partial_t)\delta n(x - vt))^S\,\vec{E} \simeq -\vec{E}\delta n(x - vt)n(i\partial_t)\vec{E}$, in which the operator $n(i\partial_t)$ acts just on the electric field E and not on the variation of the refractive index $\delta n(x - vt)$. This perturbation has the same form as the interaction Hamiltonian $\mathcal{H}_I$ considered in Ref. [17], cf. Eq. (59). In the present case $\delta n(x - vt)$ plays the role of $\xi(\vec{r},t)$ and the electric field of $\hat{\vec{\Pi}}$. These considerations allows us to apply the perturbative scheme of Ref. [17]. The expression of the electric field E is (see Ref. [21], Eq. (31), coherently adapted to the notation of Ref. [17]),

$$\begin{aligned}\vec{E}(\vec{r},t) = i\sum_{\vec{k}\mu}\left(\frac{\omega}{2V}\right)^{1/2}\frac{1}{n(\omega)n_g(\omega)} \\ \times[a_{\vec{k}\mu}(t)e^{i\vec{k}\cdot\vec{r}} - a^\dagger_{\vec{k}\mu}(t)e^{-i\vec{k}\cdot\vec{r}}]\vec{e}_{\vec{k}\mu},\end{aligned} \tag{21}$$

where $n_g(\omega) = \frac{d(n(\omega)\omega)}{d\omega} = n(\omega) + \omega\frac{dn(\omega)}{d\omega} = \frac{c}{v_g(\omega)}$ and $\underline{k} = (\vec{k},\omega) = (\vec{k},ck,n(\omega))$, with $k = |\vec{k}|$ and $\vec{e}_{\vec{k}} = \vec{k}/k$. The action of the operator $n(i\partial_t)$ on the electric field $\vec{E}$ is

$$\begin{aligned}n(i\partial_t)\vec{E} &= n(i\partial_t)\int e^{-i\omega_k t}E_\omega dk \\ &= \int n(\omega)E_\omega dk,\end{aligned} \tag{22}$$

where E_ω are the Fourier modes in the expansion [Eq. (21)] of the electric field. The operator $n(i\partial_t)$ acts on the integrand and can be expanded in power series in $i\partial_t$. The temporal derivatives act just on the exponential and one obtains a power series in ω that resumed gives $n(\omega)$, see Ref. [19]. Thus, inserting Eq. (22) in the expression of the interaction Hamiltonian, the number of particles of momentum $\vec{k}_1$ and polarization μ_1 per unit of volume generated by the disturbance $\mathcal{H}_I$ turns out to be

$$\begin{aligned}N_{\mathbf{k}_1\mu_1} &= \langle\hat{N}_{\mathbf{k}_1\mu_1}\rangle = \langle\psi(t\to-\infty)|\hat{N}_{\mathbf{k}_1\mu_1}|\psi(t\to\infty)\rangle \\ &= \int d^4x_1\int d^4x_2\langle 0|\mathcal{H}_I(x_1)\hat{N}_{\mathbf{k}_1\mu_1}\mathcal{H}_I(x_2)|0\rangle,\end{aligned} \tag{23}$$

where $\hat{N}_{\mathbf{k}_1\mu_1} = \hat{a}^\dagger_{\vec{k}_1\mu_1}\hat{a}_{\vec{k}_1\mu_1}$ is the number operator and $\psi(t\to\pm\infty)$ are the free field, i.e., the solutions of the equation of motion when the interaction is switched off. Actually, we can suppose that the interaction is present just for a finite interval of time and far from this interval the dynamics is governed by the free Hamiltonian. To compute the vacuum expectation value in Eq. (23) we use Eq. (21), with the fields evolving freely, i.e., $a_{k\mu}(t) = a_{k\mu}e^{-i\omega t}$, and, defining $f(k) := \left(\frac{\omega}{2V}\right)^{1/2}\frac{1}{n(\omega)n_g(\omega)}$, we obtain the expression,

$$\begin{aligned}N_{\mathbf{k}\mu} = \int d^4x_1d^4x_2\langle 0|\sum_{\substack{\vec{k}_1\mu_1,\vec{k}_2\mu_2,\\ \vec{k}_3\mu_3,\vec{k}_4\mu_4}} f(k_1)f(k_2)f(k_3)f(k_4) \\ \times\hat{a}_{\vec{k}_1\mu_1}\vec{e}_{\vec{k}_1\mu_1}\hat{a}_{\vec{k}_2\mu_2}\vec{e}_{\vec{k}_2\mu_2}\hat{a}^\dagger_{\vec{k}\mu}\hat{a}_{\vec{k}\mu}\hat{a}^\dagger_{\vec{k}_3\mu_3}\vec{e}_{\vec{k}_3\mu_3}\hat{a}^\dagger_{\vec{k}_4\mu_4}\vec{e}_{\vec{k}_4\mu_4} \\ \times\delta n(\underline{x}_1)\delta n(\underline{x}_2)n(\omega_2)n(\omega_4)e^{-i(k_2+k_1)x_1}e^{i(k_3+k_4)x_2}|0\rangle,\end{aligned} \tag{24}$$

where the argument $\underline{x}$ of δn is a four-vector and, in our particular case, it depends just on x and t as $x - vt$. We indicate with a tilde the four-dimensional Fourier transform $\tilde{g}(\vec{k},\frac{ck}{n_0}) = \int dtdxdydz\, g(\vec{x},t)e^{i\vec{k}\cdot\vec{x}-i\frac{ck}{n_0}t}$ and, using the commutation rules for the operators a_k and $a_k^\dagger$, $[a_{k_1,\mu_1},a^\dagger_{k_2,\mu_2}] = \delta(k_1 - k_2)\delta_{\mu_1,\mu_2}$, we obtain,

$$N_{\mathbf{k}_1\mu_1} = f(k_1)^2 \sum_{\vec{k}_2\mu_2} \widetilde{\delta n}(k_1 + k_2)^2 f(k_2)^2 [n(\omega_1) + n(\omega_2)]^2 \times \left(e_{\vec{k}_1\mu_1}\cdot e_{\vec{k}_2\mu_2}\right)^2. \quad (25)$$

The space-time dependence of the perturbation dn is of the form $\delta n(t,x,y,z) \equiv \delta n(x - vt,y,z)$. Hence, using the variables $u = x - vt$, $w = x + vt$, the Fourier transform of δn is

$$\widetilde{\delta n}(\underline{k}_1 + \underline{k}_2) = \frac{2\pi}{v}\delta\left(k_{1x} + k_{2x} - \frac{c}{v}\left[\frac{k_1}{n(\omega_1)} + \frac{k_2}{n(\omega_2)}\right]\right) \times \int du\, dy\, dz \delta n(u,y,z) e^{i(k_{1x}+k_{2x})u + i(k_{1y}+k_{2y})y + i(k_{1z}+k_{2z})z}. \quad (26)$$

A. Superluminality emission cones

As for the nondispersive case, this last result is very meaningful from a physical point of view. The support of the δ distribution gives precise conditions for the possible states of the emitted particles. First, we analyze the condition given by the δ function in the nondispersive case. Its argument gives the constraint,

$$\left(k_{1x} - \frac{c}{vn_0}k_1\right) + \left(k_{2x} - \frac{c}{vn_0}k_2\right) = 0. \quad (27)$$

This equation implies that whenever $k_{1x}/k_1 > c/(vn_0)$, the second photon must satisfy $k_{2x}/k_2 < c/(vn_0)$, i.e., from every pair of emitted photons, one photon is emitted inside the Cerenkov cone, $\theta_0 = \arccos(c/vn_0)$ (anomalous Doppler region, see Fig. 1), and the other is emitted outside the cone, in the normal Doppler region.

In the dispersive case we cannot always identify distinct cones of emission for the photons as before. The δ function gives the following condition:

$$\left(k_{1x} - \frac{c}{vn(\omega_1)}k_1\right) + \left(k_{2x} - \frac{c}{vn(\omega_2)}k_2\right) = 0. \quad (28)$$

Similarly to the nondispersive case, this equation implies that whenever $k_{1x}/k_1 > c/[vn(\omega_1)]$, the second photon must satisfy $k_{2x}/k_2 < c/[vn(\omega_2)]$. In terms of emission angles for the two photons, we find $\theta_1 < \arccos\{c/[vn(\omega_1)]\}$ and $\theta_2 > \arccos\{c/[vn(\omega_2)]\}$. Therefore, if $\arccos\{c/[vn(\omega_1)]\} > \arccos\{c/[vn(\omega_2)]\}$, the two cones overlap and, if $\arccos\{c/[vn(\omega_1)]\} < \arccos\{c/[vn(\omega_2)]\}$, there is a gap between them. In the first case, there is a region in which both photons can be emitted (differing from the nondispersive case), whereas in the second case there is a region in which no photon at all can be emitted. The two cases are shown in Figs. 2(a) and 2(b), respectively. The nondispersive case is obtained in the limiting situation in which $\arccos\{c/[vn(\omega_1)]\} = \arccos\{c/[vn(\omega_2)]\}$.

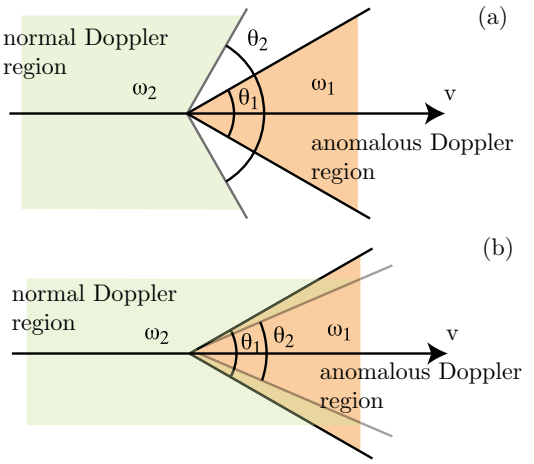

FIG. 2. (Color online) Schematical representation of correlated photon pair emission from a superluminal perturbation moving with velocity v in the presence of dispersion: the Cerenkov cone is split into two and, depending on the medium dispersion and frequency of emitted photons, regions in which no photons or both photons are emitted may appear. For the case of normal dispersion (refractive increases with increasing frequency), the figure shows the situation for $\omega_1 < \omega_2$ (a) and $\omega_1 > \omega_2$ (b).

1. Gaussian shape of the perturbation

We now focus attention on the problem of determining the actual number of emitted photons, starting from the assumption of a Gaussian shape for the refractive-index perturbation $\delta n = \eta e^{-\frac{1}{2\sigma^2}[(x-vt)^2+y^2+z^2]}$. This form for the perturbation is what one may expect when a local refractive-index variation is induced by a laser pulse through the nonlinear Kerr effect. Indeed, laser pulses typically have a Gaussian-shaped intensity, I, profile along both longitudinal and transverse rdinates so $\delta n_2 I$, where n_2 is the nonlinear Kerr index, will have the same form. A typical value for η, for example, in fused silica glass, is $\sim$0.001 where $n_2 \sim 3\times10^{-16}$ cm^2/W and we take $I \sim 3\times10^{12}$ W/cm^2. Inserting this δn profile in Eq. (25), using $\sum_{\vec{k}} \to V\int d^3\vec{k}\frac{1}{(2\pi)^3}$, and summing over the polarization states μ_1 and μ_2, using $\sum_{\lambda_1,\lambda_2}(e_{\vec{k}_1\mu_1}\cdot e_{\vec{k}_2\mu_2})^2 = \frac{k_1^2k_2^2+(\vec{k}_1\cdot\vec{k}_2)^2}{k_1^2k_2^2}$, we obtain,

$$N_{\mathbf{k}_1} = \frac{\sigma^6\eta^2\pi^2}{v^2V}\frac{\omega_1}{n^2(\omega_1)n_g^2(\omega_1)}\int d^3\vec{k}_2 e^{-\sigma^2|\vec{k}_1+\vec{k}_2|^2}\frac{\omega_2}{n^2(\omega_2)n_g^2(\omega_2)} \times [n(\omega_1)+n(\omega_2)]^2\left(\frac{k_1^2k_2^2+(\vec{k}_1\cdot\vec{k}_2)^2}{k_1^2k_2^2}\right) \times \left\{\delta[k_{1x}+k_{2x}-\frac{1}{v}(\omega_1+\omega_2)]\right\}^2. \quad (29)$$

Note that in the nondispersive limit, i.e., $\frac{dn(\omega)}{d\omega} = 0$, the expression for the number of emitted particles N_{k_1} reduces to Eq. (3).

2. *Hyperbolic tangent shape of the perturbation*

We can consider another shape for the perturbation of the refractive index. In particular, let us focus on a profile given by a hyperbolic tangent function. This allows us to investigate how the particular geometry of the perturbation affects the maximum of the wavelengths and the number of emitted particles. Moreover, a tanh shape may arise if, for example, the dominant refractive variation is related to plasma generated through multiphoton or tunneling ionization by an intense laser pulse. Intense laser pulses may indeed efficiently ionize the medium within the first few optical cycles and, thus, create a very steep moving plasma front followed by a nearly constant plasma density that will decay (through electron recombination) over time scales of the order of ∼100 fs in condensed media or ∼1 ns in gaseous media [22]. This situation, therefore, may be adequately approximated by a tanh-like function. We also note that a plasma front will locally reduce the refractive index ($\delta n < 0$) as opposed to the Kerr effect that will usually increase the refractive index ($\delta n > 0$). Yet the result of the calculations depends not on the sign of δn but only on its amplitude, velocity, and physical dimensions.

The shape of the perturbation, therefore, is taken as

$$\delta n = \eta \tanh \frac{x - vt}{\sigma_x} e^{-\frac{y^2}{2\sigma_y^2}} e^{-\frac{z^2}{2\sigma_z^2}}.$$

Again, we use the variables $u = x - vt$, $w = x + vt$, and y and z unchanged. Repeating the same computation as above, we obtain,

$$\begin{aligned} N_{\mathbf{k}_1} = {} & \frac{\sigma_x^2\sigma_y^2\sigma_z^2\eta^2\pi^2}{v^2 V}\frac{\pi}{2}\frac{\omega_1}{n^2(\omega_1)n_g^2(\omega_1)}\int d^3\vec{k}_2 \frac{\omega_2}{n^2(\omega_2)n_g^2(\omega_2)} \\ & \times \operatorname{csch}^2\left[\frac{\pi\sigma_x}{2}(k_{1x}+k_{2x})\right] e^{-\sigma_y^2(k_{1y}+k_{2y})^2} e^{-\sigma_z^2(k_{1z}+k_{2z})^2} \\ & \times [n(\omega_1)+n(\omega_2)]^2 \left(\frac{k_1^2k_2^2 + (\vec{k}_1\cdot\vec{k}_2)^2}{k_1^2k_2^2}\right) \\ & \times \left[\delta\left(k_{1x}+k_{2x}-\frac{1}{v}(\omega_1+\omega_2)\right)\right]^2. \end{aligned} \tag{30}$$

Form these relations for the total emitted photon numbers it is immediately apparent that it is advantageous to keep a large a perturbation as possible with each of the longitudinal and transverse dimensions $\sigma_{x,y,z}$ contributing equally in the multiplicative prefactor. As shown below, it turns out that the tanh profile emits roughly half the number of photons of a dimensionally similar Gaussian perturbation, indicating that the main role is played by the transient switch-on and -off of the perturbation. We also note the dependence on the group refractive index at the emission frequency. As we shall discuss below, this allows an additional degree of freedom for enhancing or controlling the photon emission process.

B. Numerical analysis: Gaussian shape

The nontrivial dispersion relation appearing in Eq. (29) makes the dispersive case more intricate to analyze, even numerically, than the nondispersive one. We perform the numerical analysis in fused silica where, for completeness, we show the full dispersion law given by the Sellmeier relation [23],

$$n(\lambda) = \mathrm{Re}\left[1 + \frac{a_1\lambda^2}{\lambda^2 - l_1^2} + \frac{a_2\lambda^2}{\lambda^2 - l_2^2} + \frac{a_3\lambda^2}{\lambda^2 - l_3^2}\right]^{1/2}, \tag{31}$$

where

$$\begin{aligned} a_1 &= 0.473\,115\,591, & l_1 &= 0.012\,995\,717\,0, \\ a_2 &= 0.631\,038\,719, & l_2 &= 4.128\,092\,20 \times 10^{-3}, \\ a_3 &= 0.906\,404\,498, & l_3 &= 98.768\,532\,2. \end{aligned}$$

As in the nondispersive case, the δ distribution in Eq. (29) gives a constraint that furnishes a relation between the momenta of the produced particles. In principle, a component of the momentum, say k_{2x}, could be expressed as a function of the other ones, so by integrating over k_{2y} and k_{2z} one could find explicitly the function $N_{\vec{k}_1}$ giving the distribution of the produced particles as a function of the momentum. However, for a generic dispersion law, the constraint cannot be analytically solved. We, therefore, study the critical points of the integrand of Eq. (29) that we will call N_{k_1,k_2}. This is a function of five variables, because the six components of the momenta are not all independent due to the constraint given by the δ. The symmetry of the problem allows us to restrict the analysis to the planes $k_{1z} = 0$ and $k_{2z} = 0$, reducing the number of variables to three. This function describes the distribution of emitted couples as function of the momenta k_1 and k_2. Its maxima show the momenta of the couple of particles emitted with highest probability. Therefore, the effective number of emitted particles can be found integrating this distribution. We note that the maximum of the function N_{k_1,k_2} is located around $\theta_1 = 0$ and $\theta_2 = \pi$. Indeed, in Eq. (29) all factors depend on $\vec{k}_1$ and $\vec{k}_2$ by their modulus except for the terms $|\vec{k}_1 + \vec{k}_2|^2$ and $(\vec{k}_1\cdot\vec{k}_2)^2$, depending on the relative orientation between the two wave vectors. For fixed k_1 and k_2, the function N_{k_1,k_2} is maximum for small $|\vec{k}_1 + \vec{k}_2|^2$ and large $(\vec{k}_1\cdot\vec{k}_2)^2$. Let $\vec{k}_1 = (k_{1x},k_{1y},0) = (k_1\cos\theta_1, k_1\sin\theta_1, 0)$ and $\vec{k}_2 = (k_{2x},k_{2y},0) = (k_2\cos\theta_2, k_2\sin\theta_2, 0)$, then

$$\begin{aligned} |\vec{k}_1 + \vec{k}_2|^2 &= k_1^2 + k_2^2 + 2k_1k_2\cos(\theta_2 - \theta_1) \\ &\geqslant k_1^2 + k_2^2 - 2k_1k_2, \\ (\vec{k}\cdot\vec{k}')^2 &= [k_1k_2\cos(\theta_2 - \theta_1)]^2 \leqslant k_1^2k_2^2. \end{aligned}$$

The two conditions are both satisfied for $\theta_2 - \theta_1 = \pi$, i.e., the two vectors point in opposite directions. The condition given by the δ function in Eq. (29) is $k_{1x} + k_{2x} - \frac{c}{v}(\frac{k_1}{n(\omega_1)} + \frac{k_2}{n(\omega_2)}) = 0$ that can be rewritten as $k_1\cos\theta_1 - k_2\cos\theta_1 - \frac{c}{v}\frac{k_1}{n(\omega_1)} - \frac{c}{v}\frac{k_2}{n(\omega_2)} = 0$, where θ_1 is the angle between $\vec{k}_1$ and the x axis and, consequently, $\pi + \theta_2$ the angle between k_2 and the x axis. As observed before, the maximum of Eq. (29) depends only on k_1, k_2, and $\vec{k}_1\cdot\vec{k}_2$, Thus, at the maxima we have

$$\begin{aligned} & \frac{d}{d\theta_1}[N_{k_1,k_2}(k_1,k_2,\vec{k}_1\cdot\vec{k}_2) + \lambda g(k_1,k_2,\theta_1)] \\ & \quad = \frac{d}{d\theta_1}\lambda g(k_1,k_2,\theta_1) = \lambda(k_1 - k_2)\sin\theta_1 = 0, \end{aligned}$$

where λ is a Lagrange multiplier. With k_1 and k_2 in general being not equal and $\lambda \neq 0$, we, therefore, have $\theta_1 = 0$. We also

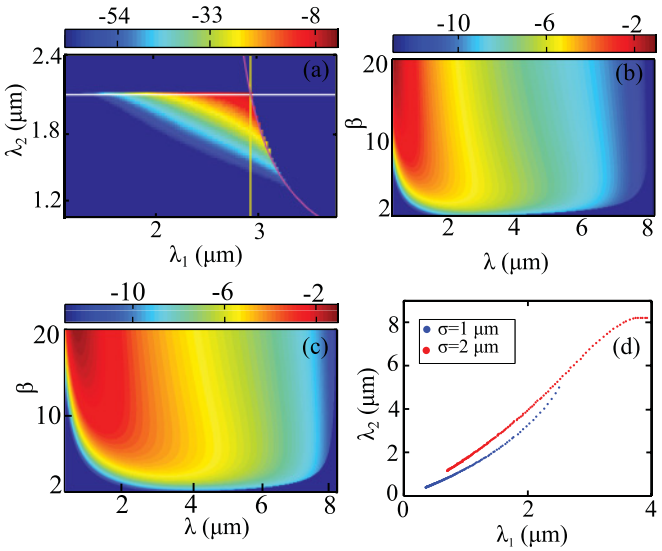

FIG. 3. (Color online) (a) $\mathrm{Log}_{10} N_{\lambda_1,\lambda_2}$ for k_{1x} corresponding to the maximum. (b) Maxima of $\log_{10} N_{\lambda_1,\lambda_2}$ for $\theta_1 = 0, \theta_2 = \pi$, and $\sigma = 1$ μm. (c) Maxima of $\log_{10} N_{\lambda_1,\lambda_2}$ for $\theta_1 = 0$, $\theta_2 = \pi$, and $\sigma = 2$ μm. (d) Relation between the wavelengths of the emitted couples for β increasing from 2, in the right part of the figure, to 20, in the left part of the figure.

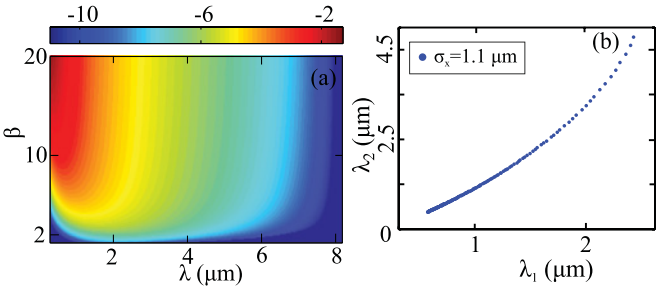

FIG. 4. (Color online) (a) $\mathrm{Log}_{10} N_{\lambda_1,\lambda_2}$ for $\theta_1 = 0, \theta_2 = \pi$ and for a hyperbolic tangent shape of the perturbation. (b) Correlated photon wavelengths for β increasing from 2 (top right point) to 20 (bottom left point).

verified numerically that, indeed, the maximum of N_{k_1,k_2} is at $\theta_1 = 0$: We visualize this in Fig. 3(a), which shows an example ($\sigma = 2$ and $\beta = 5$) of the distribution of photon numbers in a logarithmic scale. The two straight lines correspond to the condition $k_1^2 = k_{1x}^2$ and $k_2^2 = k_{2x}^2$ and the curve represents the relation between λ_1 and λ_2 given by the δ function in Eq. (29). As discussed, these three curves intersect at the maximum of N_{k_1,k_2}, implying that, indeed, maximum emission occurs along the propagation direction $\theta_1 = 0$.

We perform the numerical analysis for perturbations with radius $\sigma = 1$ μm and $\sigma = 2$ μm and for increasing values of β. As explained, to give an estimation of the number of emitted couples for every single PDM we have to evaluate the integrand of the Eq. (29), i.e., $N_{k_1,k_2} := dN/(d\Omega d\Omega' dk dk')$. In the computation the value of $\delta(0)$ has been approximated with $L/(2\pi)$ [see Eq. (26)]. In the following we report all photon numbers in the function of wavelength rather than wave vector (thus indicated as N_{λ_1,λ_2}) and integrated over the azimuthal angles φ_1 and φ_2.

Figures 3(b) and 3(c) show the calculated photon numbers N_{λ_1,λ_2} in logarithmic scale for the value of λ_2 at which emission is maximum and for $\eta = 0.001$, two different values of the perturbation size, $\sigma = 1$ and 2 μm, respectively. Figure 3(d) shows both wavelengths $\lambda_1 = \lambda_{1\mathrm{max}}$ and $\lambda_2 = \lambda_{2\mathrm{max}}$ at which emission is maximum and for $2 < \beta < 20$. At lowest β, λ_1 and λ_2 have the largest values and monotonically decreases and β increases. These points are also shown for the two values of σ considered, 1 μm (blue dots) and 2 μm (red dots). We observe that the photon emission peaks at wavelengths $\lambda_{1\mathrm{max}}$, which increases with the perturbation diameter. We also note that, as in the nondispersive case [15], $\lambda_{1\mathrm{max}}$ and $\lambda_{2\mathrm{max}}$ decrease from the midinfrared region into the visible region as β, i.e., the perturbation velocity, increases. However, differing from the nondispersive case, we underline that, in general, $\lambda_{1\mathrm{max}}$ and $\lambda_{2\mathrm{max}}$ differ, i.e., the photons are correlated but at different wavelengths. However, for increasing β this difference becomes smaller with $\lambda_{1\mathrm{max}} \to \lambda_{2\mathrm{max}}$ as $\beta \to \infty$ (Fig. 3(d) and 4(b)).

Some numerical values of N_{λ_1,λ_2} from these graphs are given in Table I [(a) and (b)]. An estimation of the actual number of emitted particles can be obtained by integrating the function N_{λ_1,λ_2} over λ, θ_1, and θ_2: This furnishes, for $\eta =$

TABLE I. Maxima of N_{λ_1,λ_2} for increasing β and two values of σ. Numbers in square brackets denote powers of 10.

(a) $\sigma = 1$ μm				(b) $\sigma = 2$ μm			
β	$\lambda_{1\mathrm{max}}$ m	$\lambda_{2\mathrm{max}}$ m	N_{λ_1,λ_2}	β	$\lambda_{1\mathrm{max}}$ m	$\lambda_{2\mathrm{max}}$ m	N_{λ_1,λ_2}
2	2.51[−6]	4.98[−6]	6.13[−7]	2	3.93[−6]	7.02[−6]	4.14[−8]
3	1.93[−6]	3.06[−6]	6.68[−6]	3	3.50[−6]	5.38[−6]	2.14[−6]
4	1.54[−6]	2.17[−6]	3.01[−5]	4	2.95[−6]	4.11[−6]	1.27[−5]
5	1.26[−6]	1.66[−6]	9.35[−5]	5	2.49[−6]	3.26[−6]	4.28[−5]
6	1.08[−6]	1.36[−6]	2.33[−4]	6	2.13[−6]	2.68[−6]	1.11[−4]
7	0.94[−6]	1.15[−6]	5.02[−4]	7	1.87[−6]	2.69[−6]	2.44[−4]
8	0.83[−6]	0.99[−6]	8.73[−4]	8	1.65[−6]	1.96[−6]	4.80[−4]
9	0.75[−6]	0.87[−6]	1.74[−3]	9	1.48[−6]	1.73[−6]	8.69[−4]
10	0.68[−6]	0.78[−6]	2.91[−3]	10	1.35[−6]	1.54[−6]	1.47[−3]
15	0.47[−6]	0.52[−6]	2.09[−2]	15	0.92[−6]	1.00[−6]	1.11[−2]
20	0.36[−6]	0.39[−6]	8.19[−2]	20	0.70[−6]	0.75[−6]	4.63[−2]

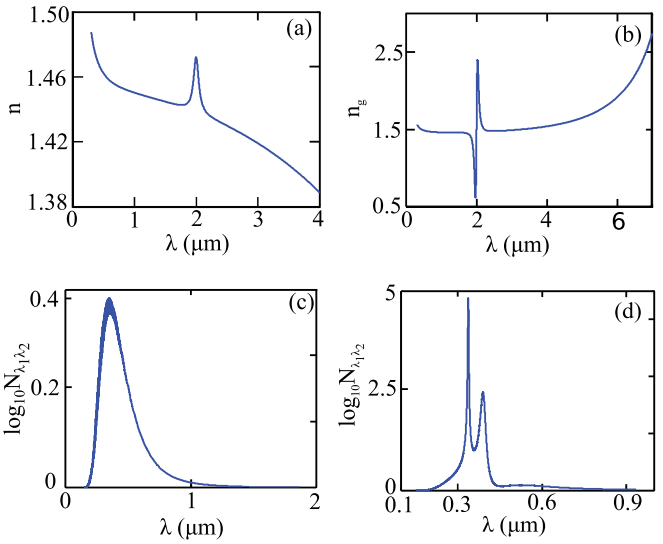

FIG. 5. (Color online) Dispersion law (a) and group index (b) for the modified dispersion law of the fused silica. (c) $\mathrm{Log}_{10}N_{\lambda_1,\lambda_2}$ for the standard dispersion law of the fused silica. (d) $\mathrm{Log}_{10}N_{\lambda_1,\lambda_2}$ for the modified dispersion law of the fused silica.

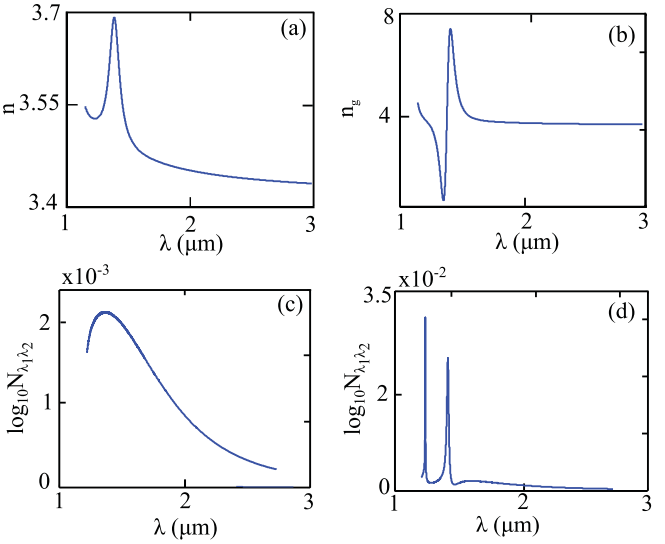

FIG. 6. (Color online) Dispersion law (a) and group index (b) for the modified dispersion law of the silicon. (c) $\mathrm{Log}_{10}N_{\lambda_1,\lambda_2}$ for the standard dispersion law of the silicon. (d) $\mathrm{Log}_{10}N_{\lambda_1,\lambda_2}$ for the modified dispersion law.

0.001, $\sigma = 1$ μm, $\beta = 20$, and a 5-cm propagation distance, a number of emitted photons for every PDM in an angle of 30° of $\sim 3 \times 10^{-4}$.

C. Numerical analysis: Hyperbolic tangent shape

We perform a similar numerical analysis for a hyperbolic tangent shape of the perturbation of the refractive index by studying the integrand of Eq. (30). Adapting the previous argument to this case, we search its maxima in the direction of the propagation of the PDM, i.e., for $\theta = 0$. We assume a perturbation with dimensions $\sigma_x = 1.1$ μm and $\sigma_y = \sigma_z = 1$ μm and $\eta = 0.001$. An estimation similar to the Gaussian case, for $\beta = 20$ and a 5-cm propagation distance, gives a number of emitted photons for every PDM in an angle of 30° of $\sim 1.5 \times 10^{-4}$.

D. Fast light

We now return to a feature outlined earlier on, i.e., the dependence of the photon emissivity on the group index at the emitted frequencies [see, e.g., Eq. (29)]. From our equations it is clear that by a reduction in the group velocity at ω_1 and/or ω_2 may greatly influence the actual number of emitted photons at both frequencies. Group velocities exceeding the speed of light have been observed in several experiments [24–28], whereby the medium is chosen either to have an absorption resonance close to the frequency of interest or is structurally modified, e.g., into Bragg grating structures so the dispersion curve is strongly modified (without absorption). This property, therefore, can be exploited to effectively engineer the (dispersion properties of the) vacuum states, increasing the number of emitted photons and, moreover, providing an additional tool for investigating the correlation properties of the produced couples. We emulate such superluminal group velocities by introducing a simple Lorentzian correction on top of a background Sellmeier relation. We, therefore, obtain a dispersion law with a narrow peak whose maximum slope is placed in correspondence to the point of the highest photon emission for a medium characterized only by the background dispersion. We give an example of such a modified dispersion law for the fused silica in Fig. 5(a) and the corresponding group index, $n_g(\omega)(\lambda(\omega)) - \lambda(\omega)\frac{dn(\lambda)}{d\lambda}$, in Fig. 5(b).

We then perform the analysis for a PDM of Gaussian shape with $\eta = 0.001$, $\sigma = 1$ μm and traveling at $\beta = 20$ in such a medium. In Fig. 5(c) we show the distribution of the emitted couples in a medium with the background dispersion law and in Fig. 5(d) the distribution produced by the same perturbation in a medium with the Lorentzian correction to the dispersion. As a first comment, we observe that the number of emitted particles increases by a factor of 10 due to the dependence of Eq. (29) on the group indices $n_g(\omega_1)$ and $n_g(\omega_2)$. Moreover, the emission spectrum is strongly distorted but, most importantly, two distinct maxima appear. These two peaks are related to enhanced emission separately at λ_1 or at λ_2. In virtue of the nature of the two emitted photons, enhancement at one wavelength will necessarily lead to enhancement at the correlated photon wavelength. Therefore, observation of these two emission peaks in an experiment could be considered as evidence of correlated photon emission from the superluminal perturbation by measuring only in the forward direction. We performed a similar analysis for the case of silicon, as this is a widely used material in optics and waveguide technology where both slow and fast light may be engineered. We obtain a similar increase of the emitted particles as shown in Fig. 6 for a perturbation of dimension $\sigma = 1$ μm and velocity $\beta = 4$.

V. CONCLUSIONS

Perturbative analysis of quantum fluctuation excitation from a traveling refractive-index perturbation indicates that emission of correlated photon pairs occurs only if $v > c/n(\omega)$. This effect bears a strong resemblance to the anomalous Doppler effect and, in this sense, represents the first detailed analysis of a setting in which the effect may actually be ob-

served. The number of emitted photon pairs is relatively small close to the threshold $v = c/n(\omega)$ but increases significantly if v is much larger (e.g., 10–20×) than c. Our analysis fully accounts for material dispersion and, in doing so, introduces an intriguing dependence on the group index or group velocity of the emitted photons. This dependence and careful engineering of the host medium may be used to enhance photon emission by at least an order of magnitude and also provides direct evidence of correlated emission in the form of two correlated peaks in the output spectra.

From our analysis, it would seem that experiments are, indeed, feasible. Refractive-index perturbations of the order of those used in this work, $\eta \sim 0.001$, may be obtained by focusing laser pulses in fused silica or other nonlinear media and higher values have been observed. According to our results, this would result in a photon-pair emission rate of $\sim 10^{-6}$ pairs/pulse at $\beta = 20$ in a 5-mm-long waveguide, i.e., ~ 1 photon per second if a MHz-repetition-rate laser is used. These numbers may be increased by an order of magnitude or more, e.g., by using fast-light media or higher PDM amplitudes. The high velocities used here for the perturbation may be obtained experimentally by sending an extended (approximately "plane wave") laser pulse at an angle onto the host medium that could be, for example, a waveguide (see Fig. 7). The pulse would intersect the waveguide with an angle θ and the Kerr effect would create a PDM only at the intersection point that travels with speed $c/\cos\theta$ (if we approximate the refractive index of air ~ 1). Therefore, an incidence angle of $\sim 80^\circ$–85° (i.e., close to normal incidence on the waveguide) would guarantee $\beta \sim 5$–20. We note that a similar approach has actually been used in previous pioneering experiments in which a dc field was converted to terahertz radiation by a superluminal laser pulse excitation of an array of biased capacitors [29]. In our case, we are exciting a superluminal PDM in a dielectric medium and correlated photon pairs would be generated and collected from the two ends of the waveguide.

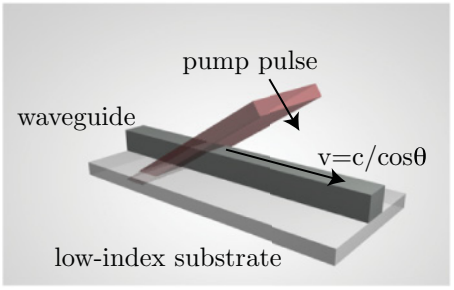

FIG. 7. (Color online) Schematical representation of an experimental layout for creating a superluminal refractive-index perturbation in a waveguide.

ACKNOWLEDGMENTS

The authors thank T. Krauss and G. Ortenzi for fruitful discussions. F.D.P. acknowledges financial support from l'Universitá dell'Insubria and Fondazione Cariplo, Univercomo, and Banca del Monte di Lombardia.

[1] J. Schwinger, Phys. Rev. **82**, 664 (1951).
[2] S. W. Hawking, Commun. Math. Phys. **43**, 199 (1975).
[3] W. G. Unruh, Phys. Rev. Lett. **46**, 1351 (1981).
[4] C. Barceló, S. Liberati, and M. Visser, Living Rev. Relativity **14**, 3 (2011).
[5] T. G. Philbin, C. Kuklewicz, S. Robertson, S. Hill, F. König, and U. Leonhardt, Science **319**, 1367 (2008).
[6] F. Belgiorno, S. L. Cacciatori, M. Clerici, V. Gorini, G. Ortenzi, L. Rizzi, E. Rubino, V. G. Sala, and D. Faccio, Phys. Rev. Lett. **105**, 203901 (2010).
[7] E. Rubino *et al.*, New J. Phys. **13**, 085005 (2011).
[8] S. A. Fulling *et al.*, Proc. R. Soc. London A **348**, 393 (1976).
[9] M. V. Nezlin, Usp. Fiz. Nauk **120**, 481 (1976).
[10] V. L. Ginzburg *et al.*, Usp. Fiz. Nauk **153**, 633 (1987).
[11] V. L. Ginzburg, Phys. Usp. **39**, 973 (1996).
[12] V. L. Ginzburg, *Applications of Electrodynamics in Theoretical Physics and Astrophysics* (Gordon & Breach Science Publishers, London, 1989).
[13] I. Alexeev, K. Y. Kim, and H. M. Milchberg, Phys. Rev. Lett. **88**, 073901 (2002).
[14] F. Bonaretti *et al.*, Opt. Express **17**, 9804 (2009).
[15] F. Belgiorno, S. L. Cacciatori, G. Ortenzi, V. G. Sala, and D. Faccio, Phys. Rev. Lett. **104**, 140403 (2010).
[16] P. W. Milonni, *Fast Light, Slow light and Left-Handed Light* (Institute of Physics, New York, 2005).
[17] R. Schutzhold, G. Plunien, and G. Soff, Phys. Rev. A **58**, 1783 (1998).
[18] Note that in Ref. [15] there was a misprint in the numerical constant beyond Eq. (3) of a factor 2^3.
[19] T. G. Philbin, Phys. Rev. A **83**, 013823 (2011).
[20] H. Weyl, *Theory of Groups and Quantum Mechanics* (Dover, New York, 1931).
[21] P. W. Milonni, J. Mod. Opt. **42**, 10 1991 (1995).
[22] A. Couairon *et al.*, Phys. Rep. **441**, 47 (2007).
[23] G. P. Agrawal, *Nonlinear Fibre Optics* (Academic Press, New York, 1989).
[24] J. F. Galisteo-Lopez *et al.*, Opt. Express **15**, 15342 (2007).
[25] R. W. Boyd *et al.*, Science **326**, 5956 (2009).
[26] D. R. Solli, C. F. McCormick, C. Ropers, J. J. Morehead, R. Y. Chiao, and J. M. Hickmann, Phys. Rev. Lett. **91**, 143906 (2003).
[27] L. J. Wang *et al.*, Nature **406**, 277 (2000).
[28] Q. Li *et al.*, Opt. Express **17**, 933 (2009).
[29] D. Hashimshony, A. Zigler, and K. Papadopoulos, Phys. Rev. Lett. **86**, 2806 (2001).